Annals of Hematology (2024) 103:1241–1254
https://doi.org/10.1007/s00277-023-05590-y

ORIGINAL ARTICLE

Investigation of fatty acid metabolism in chronic lymphocytic leukemia to guide clinical outcome and therapy

Bihui Pan[1,2,3] · Zhangdi Xu[1,2,3] · Kaixin Du[1,2,3] · Rui Gao[4] · Jiale Zhang[1,2,3] · Hua Yin[1,2,3] · Haorui Shen[1,2,3] · Jinhua Liang[1,2,3] · Yue Li[1,2,3] · Li Wang[1,2,3] · Jianyong Li[1,2,3] · Wei Xu[1,2,3] · Jiazhu Wu[1,2,3]

Received: 11 November 2023 / Accepted: 15 December 2023 / Published online: 27 December 2023

Abstract

Chronic lymphocytic leukemia (CLL) is the most common leukemia in the West. With CLL's heterogeneity, some people still develop disease refractory and relapse despite advances in treatment. Thus, early diagnosis and treatment of high-risk CLL patients is critical. Fatty acid (FA) metabolism contributes to tumorigenesis, progression, and therapy resistance through enhanced lipid synthesis, storage, and catabolism. In this study, we aimed to construct a prognostic model to improve the risk stratification of CLL and reveal the link between FA metabolism and CLL. The differentially expressed FA metabolism-related genes (FMGs) in CLL were filtered through univariate Cox regression analysis based on public databases. Functional enrichment was examined using prognostic FA metabolism-related gene enrichment analysis. CIBERSORT and single-sample gene set enrichment analysis (ssGSEA) estimated immune infiltration score and immune-related pathways. Pearson's correlation analysis investigated FA metabolism-related genes and drug sensitivity. A novel prognostic model was built using least absolute shrinkage and selection operator (LASSO) Cox algorithms. This validation cohort included 36 CLL patients from our center. We obtained CLL RNA microarray profiles from public databases and identified 15 prognostic-related FMGs. CLL patients were divided into two molecular clusters based on the expression of FMGs. The Kaplan–Meier analysis revealed a significant difference in TFS ($P < 0.001$) and OS ($P < 0.001$) between the two clusters. KEGG functional analysis showed that several pathways were enriched, including the chemokine and immune-related signaling pathways. In the training and validation cohorts, patients with higher FA metabolism-related prognostic index (FAPI) levels had worse outcomes. Finally, a novel nomogram prognostic model including CLL international prognostic index (CLL-IPI) was constructed, exhibiting reliable effectiveness and accuracy. In conclusion, we established a reliable predictive signature based on FA metabolism-related genes and constructed a novel nomogram prognostic model, supporting the potential preclinical implications of FA metabolism in CLL research.

Keywords Chronic lymphocytic leukemia · Fatty acid metabolism · Prognosis · Immune infiltration · Nomogram

Introduction

Chronic lymphocytic leukemia (CLL), the most prevalent adult leukemia in the Western World, has a wide spectrum of disease courses [1, 2]. Some patients require little or no treatment while others need immediate therapy at the time of

Bihui Pan, Zhangdi Xu, and Kaixin Du contributed equally to this work.

✉ Wei Xu
xuwei10000@hotmail.com

✉ Jiazhu Wu
wujiazhu09@sina.com

[1] Department of Hematology, The First Affiliated Hospital of Nanjing Medical University, Jiangsu Province Hospital, Nanjing 210029, China

[2] Key Laboratory of Hematology of Nanjing Medical University, Nanjing 210029, China

[3] Collaborative Innovation Center for Cancer Personalized Medicine, Nanjing 210029, China

[4] Department of Endocrinology and Metabolism, The First Affiliated Hospital of Nanjing Medical University, Nanjing, China

diagnosis. Overall survival (OS) is divergent, ranging from a few years postdiagnosis to decades as almost normal life expectancy [3]. Over the past few decades, despite the development of emerging therapeutic targets is rapidly advancing, such as BTK inhibitors, BCL-2 inhibitors, and PI3K inhibitors, CLL is still incurable [4, 5]; some patients continue to experience disease relapse and refractoriness, indicating the heterogeneity of CLL and the need to differentiate various prognosis risk groups as a way to replenish the CLL international prognostic index (CLL-IPI).

Metabolic reprogramming is a hallmark of many cancers [6]. In recent years, various metabolic alterations have been identified in hematological tumors, including glucose metabolism, nucleotide metabolism, and fatty acid (FA) metabolism [7]. FA synthesis is required for anabolic reactions such as membrane biosynthesis and the production of signaling molecules. Oxidation of FA produces more than twice the ATP yield of glucose or amino acids, making FA an important fuel [8]. On the other hand, metabolic reprogramming leads to abnormal lipid metabolism, in particular, the de novo synthesis of FA is increased by hypoxia and malnutrition. The significance of lipid metabolism in different kinds of cancers is well-recognized [9]. Wu et al. suggested that FA synthesis was considered a vital metabolism pathway in colon adenocarcinoma. Another study found that expression patterns of FA metabolism genes were associated with glioma prognosis and immunophenotype [10]. Targeting metabolism to overcome cancer drug resistance is thought as a promising therapeutic strategy for diffuse large B cell lymphoma [11]. In hematological malignancy, active FA oxidation may promote acute myeloblastic leukemia cells to survive and bone marrow adipocytes to resolve. Unlike normal B lymphocytes or other leukemia cells, CLL cells, like adipocytes, store lipids and use free FAs (FFA) to generate chemical energy, using oxidative phosphorylation of free FAs to meet the high metabolism required for proliferation need [12, 13]. Furthermore, studies have shown that high levels of FAs are rapidly internalized by CLL cells rather than glucose uptake. Higher animal fat and saturated fat intake were positively associated with CLL risk. Epidemiologic evidence also suggests that dietary fat intake significantly increases the risk of non-Hodgkin lymphomas [14]. In addition, higher animal and saturated fat intakes are positively associated with the risk of CLL in the MCC-Spain study [15]. Lipoprotein lipase (LPL) is conventionally regarded as the principal enzyme involved in lipid metabolism. Numerous studies have validated that the presence of LPL mRNA is strongly linked to unfavorable prognosis and serves as the most reliable molecular indicator of CLL [16–20]. However, fewer prognostic indicators or models for CLL exploit reprogrammed lipid metabolism except for LPL. Our team has previously investigated the association between certain metabolic indicators and the clinical manifestations and prognosis of CLL, including low cholesterol levels and low T3 syndrome, which serve as biomarkers of tumor activity [21, 22]. Currently, the FA metabolism-related gene set in CLL has not been systematically studied.

To further explore the association between CLL and FA metabolism, we filtered differentially expressed and prognostic-related FA metabolic genes in CLL based on public databases to build a novel prognostic risk model in this study. The relationship between the tumor microenvironment (TME) cell infiltration characteristics and the prediction risk rating model was also investigated. The predictive risk score approach correctly identifies CLL patients who are immunotherapy candidates. Ultimately, our research aims to build a prognostic model based on FA metabolism-related genes to improve risk stratification in CLL patients and facilitate more accurate assessment for their clinical management.

Materials and methods

Database resource collecting

The RNA microarray profiles for 151 CLL patients were extracted from the GSE22762 dataset in the Gene Expression Omnibus (GEO) database (https://www.ncbi.nlm.nih.gov/geo/) as the training cohort. The microarray data from the GSE50006 dataset including another 188 CLL patients and 32 normal samples were used to analyze differentially expressed genes (DEGs). All expression data were normalized using the "sva" R package. The data from GEO is publicly available.

Clinical sample preparation and RNA sequencing

As the validation cohort, the RNA sequencing (RNA-seq) data of thirty-six CLL patients diagnosed between 2012 and 2017 in the First Affiliated Hospital of Nanjing Medical University were enrolled. All the total RNA samples in our center were obtained from the purified $CD19^+$ B cells of CLL patients using $CD19^+$ B cells selection kit (Miltenyi Biotech, Gladbach, Germany). Sequencing libraries were prepared by NEBNext Ultra RNA Library Prep Kit for Illumina (New England Biolabs, Ipswich, MA) and sequenced by HiSeq 2500 high-throughput sequencing system. Sequences were mapped to hg38 and aligned using bowtie and blat. Obtained fragments per kilobase million (FPKM) values were normalized in log2 (FPKM + 1).

Additionally, clinical characteristics including age, sex, Binet stage, B symptoms, lymphocyte count, hemoglobin level, platelet count, lactate dehydrogenase (LDH) level, β2-microglobulin (β2-MG) level, complex karyotype, TP53 disruption, and IGHV mutation status were extracted from medical records. This study was approved by the

institutional review board of the First Affiliated Hospital of Nanjing Medical University.

Acquisition and enrichment analysis of prognostic FA metabolism-related genes

FA metabolism-related genes were gathered from three gene sets in Gene Set Enrichment Analysis (GSEA) database (http://www.gsea-msigdb.org/gsea/), including HALLMARK FA metabolism, KEGG FA metabolism, and REACTOME FA metabolism, and were provided in Table S1. Univariate Cox regression analysis was performed to identify prognostic-related genes. The *t*-test was used to distinguish the DEGs based on the GSE50006. Venn diagram was showing up the intersection genes of FA metabolism-related genes, prognostic-related genes, and DEGs. Moreover, Gene Ontology (GO) and Kyoto Encyclopedia of Genes and Genomes (KEGG) analyses were performed to explore the functional enrichment of the intersection genes via the "clusterprofiler" R package.

Unsupervised clustering for FA metabolism-related genes

Unsupervised clustering analysis was used to divide patients into two different molecular clusters based on the expression of differentially expressed FA metabolism-related genes via the "clusterprofiler" R package. Survival curves on OS time, treatment-free survival (TFS) time, and progress-free survival (PFS) time of two clusters were calculated by the Kaplan–Meier method and compared by the log-rank test with the "survminer" R package. The DEGs between two clusters were identified by "limma" R package; furthermore, the functional enrichment and tumor immune microenvironment were carried out to investigate potential biological behavior.

Tumor immune microenvironment, m6A regulators, and drug sensitivity analysis

Single-sample gene set enrichment analysis (ssGSEA) was performed to estimate the immune infiltration score of twenty-eight immune cell subtypes and thirteen immune pathways. The gene sets included in ssGSEA are listed in Table S2. The relative proportion of twenty-two infiltrating immune cell subtypes was estimated by the CIBERSORT (https://cibersort.stanford.edu/) algorithm. The expression value of immune checkpoint genes is compared between different subtypes by Wilcox test. The checkpoint genes and m6A-related gene sets are listed in Table S3. Finally, the CellMiner database (https://discover.nci.nih.gov/cellminer/home.do) was used to explore the relationship between DEGs and common FDA-approved antineoplastic drug sensitivity by a panel of 60 diverse human cancer cell lines. The half maximal inhibitory concentration (IC50) was used to predict the treatment response of the cell lines to the drugs.

Construction of the risk score prognostic model and nomogram models

Least absolute contraction and selection operator (LASSO) regression analysis was established to minimize the potential overfitting risk via the "glmnet" R package. Fifteen prognostic FA metabolism-related genes were included in the LASSO analysis, and the risk score was calculated by the formula $\sum_{i=1}^{n} \beta_i * x_i$, β represents the coefficients, and x represents the gene expression. According to the optimal cut-off value of risk score, patients were divided into a low-risk group and a high-risk group. Principal component analysis (PCA) and *t*-distributed stochastic neighbor embedding (tSNE) were used to visualize the distribution of groups through the "ggbiplot" R package. The receiver-operator characteristic curve (ROC) and corresponding area under the curve (AUC) were calculated to evaluate the prognostic ability of the risk-scoring model. A nomogram model was constructed to estimate the probability of 1-year, 3-year, and 5-year OS by the "rms" R package. The capacity for prognostic prediction was evaluated by the concordance index (*C*-index).

Statistical analysis

Statistical analyses were performed by R software (version 4.1.1) and IBM SPSS (version 21.0). Continuous variables were compared by the *t*-test or Kruskal–Wallis test. $P < 0.05$ was considered statistically significant.

Results

Identification of prognostic FA metabolism-related DEGs in CLL

FA metabolism-related genes were collected from three gene sets in GSEA; after removing duplicate genes, a total of 291 FA metabolism-related genes were acquired. Based on the GSE22762 dataset as a training cohort, 3081 genes were found to be associated with poor OS outcomes by univariate Cox regression analysis. Based on the GSE50006 dataset, 6213 statistically significant DEGs were screened by comparing the gene expression in CLL patients and normal samples. Filter conditions were set for log fold change > 0.4 and adjusted P value < 0.05. Venn diagram was showing up that there are 15 overlapping genes of FA metabolism-related genes, prognostic-related genes, and DEGs (Fig. 1A).

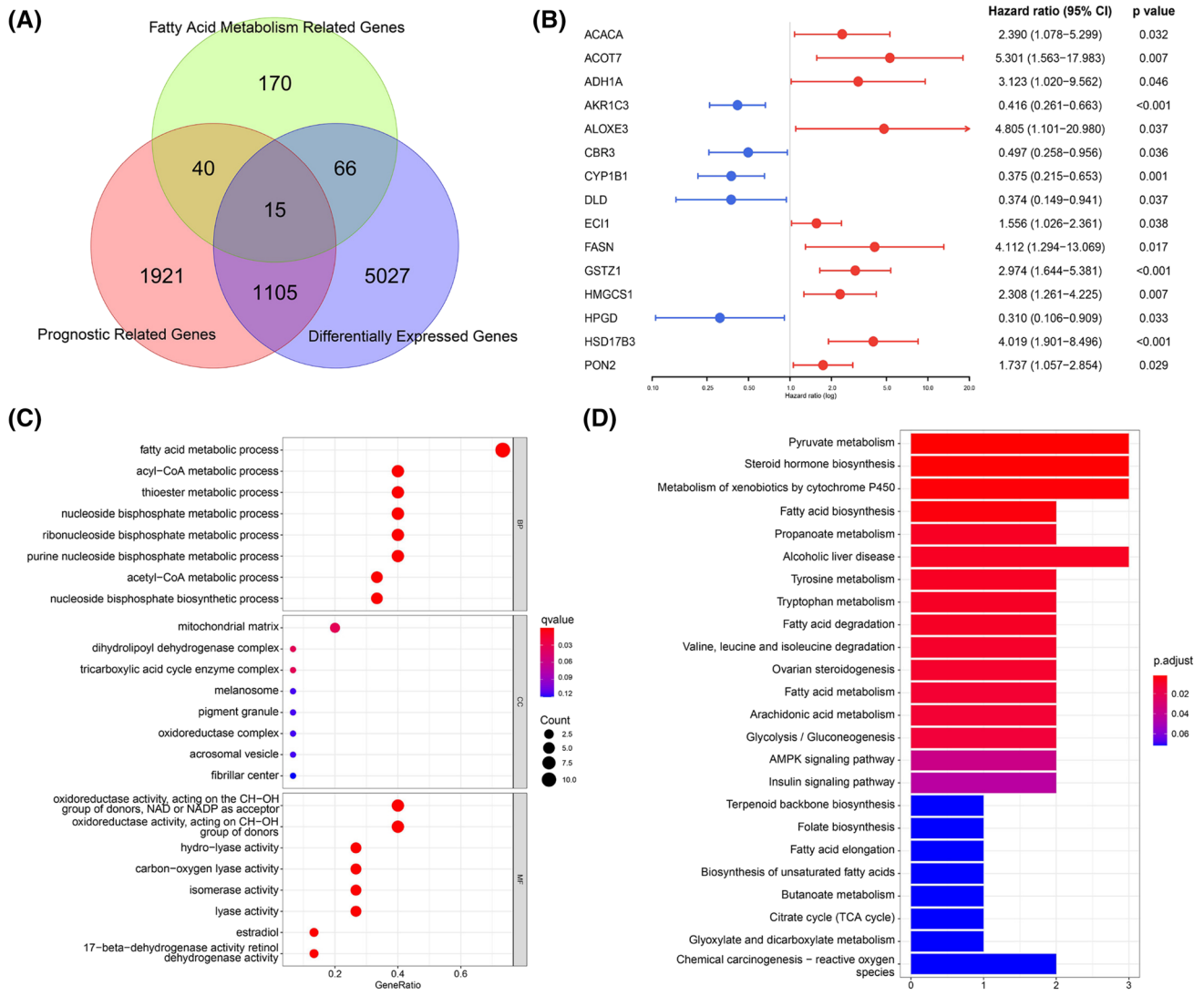

Fig. 1 Identification of prognostic FA metabolism-related DEGs in CLL. **A** Venn diagram was showing up the intersection genes of FA metabolism-related genes, prognostic-related genes, and DEGs. **B** Forest plot with hazard ratios of the univariate Cox regression analysis showing the prognostic value in the GSE22762 dataset. **C**, **D** GO and KEGG analyses of the functional enrichment of the FA metabolism-related DEGs

Among them, ten genes (ACACA, ACOT7, ADH1A, ALOXE3, ECI1, FASN, GSTZ1, HMGCS1, HSD17B3, and PON2) were correlated with poor outcomes, and five genes (AKR1C3, CBR3, CYP1B1, DLD, and HPGD) were associated with favored OS (Fig. 1B). Moreover, we used GO and KEGG analyses to explore the functional enrichment of the 15 intersection genes. GO enrichment analysis revealed that these FA metabolism-related genes were highly enriched in biological processes of FA metabolic, acyl-CoA metabolic, and thioester metabolic, enriched in molecular function of oxidoreductase activity, acting on the CH-OH group of donors, NAD or NADP as acceptor and oxidoreductase activity, acting on CH-OH group of donors (Fig. 1C). KEGG analysis found that FRGs were enriched in pyruvate metabolism, steroid hormone biosynthesis, metabolism of xenobiotics by cytochrome P450, FA biosynthesis, FA degradation, FA metabolism, as well as AMPK signaling pathway (Fig. 1D).

Two FA metabolism-related molecular clusters of CLL identified by unsupervised clustering

As shown in Fig. 2A, based on the expression of 15 overlapping genes in Fig. 1A, CLL patients were divided into two molecular clusters (Cluster 1, $n = 99$, 65.6%, and Cluster 2, $n = 52$, 34.4%). PCA and tSNE were used to visualize the distinct differences between different molecular clusters (Fig. S1A-B). The Kaplan–Meier analysis showed that

patients in Cluster 1 had statistically significantly worse TFS ($P < 0.001$) and OS ($P < 0.001$) (Fig. 2B, C). Furthermore, to investigate the difference in characterization and biological behavior between the two clusters, we performed 419 DEGs with log fold change > 0.6 and adjust P value < 0.05 (Fig. 2D). The heatmap depicting DEGs is shown in Fig. 2E. All the DEGs were used to perform KEGG and GO functional enrichment analysis to unearth potential biological functions. KEGG functional analysis showed that several pathways, including the chemokine signaling pathway, IL-17 signaling pathway, NF-κB signaling pathway, PD-L1 expression and PD-1 checkpoint pathway in cancer, and T cell receptor signaling pathway, were enriched (Fig. 2F–H). GO functional analysis showed that DEGs were significantly enriched in neutrophil activation, neutrophil-mediated immunity, and T cell activation (Fig. 2I–K).

Tumor immune microenvironment and m6A regulator analysis between different FA metabolism-related phenotypes

Considering that immune response and T cell activation pathway were enriched by KEGG and GO functional enrichment analysis, we further used two algorithms, which were ssGSEA and CIBERSORT, to estimate the infiltrating immune cell types and related immune pathways between the two clusters. The ssGSEA analysis performed that Cluster 2 patients exhibited an abundance of immune cell infiltration, including activated $CD4^+$ T cells, activated $CD8^+$ T cells, activated dendritic cells, activated killer (NK) cells, central memory $CD4^+$ T cells, central memory $CD8^+$ T cells, effector memory $CD4^+$ T cells, effector memory $CD8^+$ T cells, eosinophil, gamma delta T cells, immature dendritic cells, macrophage, mast cells, myeloid-derived suppressor cell, NK cells, NKT cells, neutrophil, plasmacytoid dendritic cells, regulatory T cells (Tregs), follicular helper T cells, type 1 T helper cell, type 17 T helper cell, and type 2 T helper cell (Fig. 3A). Additionally, the score of immune-related pathways, including APC co-inhibition, APC co-stimulation, C–C chemokine receptor (CCR), check-point, cytokine activity, inflammation-promoting, parainflammation, T cell co-inhibition, T cell co-stimulation, and type II IFN response, was higher in Cluster 2, while the score of HLA pathway was higher in Cluster 1 (Fig. 3B). Furthermore, we also used CIBERSORT algorithms to estimate the infiltrating immune cell types. Compared with patients in Cluster 1, Cluster 2 had significantly higher relative fractions of naive $CD4^+$ T cells, activated memory $CD4^+$ T cells, resting NK cells, monocytes, activated mast cells, eosinophils, and neutrophils (Fig. 3C). In addition, we compared the expression of 47 checkpoint genes between two clusters. Statistically, there were 23 genes significantly different; among them, six checkpoint genes (BTLA, CD200, CD27, CD40, CTLA4, and TNFSF9) were highly expressed in Cluster 1; contrarily, other 17 genes were dramatically upregulated in Cluster 2 (Fig. 3D). Subsequently, we compared 20 m6A-related gene expressions in different FA metabolism-related phenotypes. The results demonstrated remarkable differences in four genes, such as HNRNPC, IGF2BP2, METTL3, and YTHDF1 (Fig. 3E).

The correlation between the expression of FA metabolism-related genes and the sensitivity of chemotherapy

We used Pearson's correlation analysis to explore the relationship between 15 FA metabolism-related genes and drug sensitivity. These FA metabolism-related genes have been implicated in 99 FDA-certified drug sensitivity with P value < 0.05 (Table S4), including 8 common chemotherapeutic drugs for CLL (Fig. 4). The analysis demonstrated that increased ACOT7 expression was associated with increased drug IC50 of fludarabine and decreased IC50 of umbralisib, increased ALOXE3 expression was associated with decreased IC50 of ABT-199, increased CYP1B1 expression was associated with increased IC50 of ibrutinib and decreased IC50 of oxaliplatin, increased ECI1 expression was associated with decreased IC50 of bendamustine, and increased HMGCS1 was associated with increased drug sensitivity of dexamethasone Decadron; furthermore, as HPGD expression increased, cancer cell drug sensitivity to dexamethasone Decadron and cyclophosphamide decreased (Fig. 4).

Establishment of a novel prognostic model based on FA metabolism-related genes

Correlation analysis on 15 FA metabolism-related genes was performed to elucidate the interaction between these genes (Fig. 5A). Then, we conducted LASSO Cox regression analysis to establish the FA metabolism-related prognostic index (FAPI). Based on optimal weight coefficients (λ), four genes were identified in this novel prognostic model, comprising AKR1C3, CYP1B1, GSTZ1, and HSD17B3. The FAPI score was calculated by the formula (-0.1209) *AKR1C3 + (-0.0287) *CYP1B1 + (0.2286) *GSTZ1 + (0.2772) *HSD17B3 (Fig. 5B, C). According to the optimal cut-off values (cut-off = 2.4230), the patients could be stratified into two groups: 70 (46.36%) patients in the low-risk group and 81 (53.64%) patients in the high-risk group. Survival status, distribution of risk scores, and gene expression heatmap are shown in Fig. 5D, F, respectively. PCA and tSNE analysis illustrated that patients in different risk groups were well separated into two different groups (Fig. 5G, H). The Kaplan–Meier analysis showed that patients with high FAPI levels had a statistically

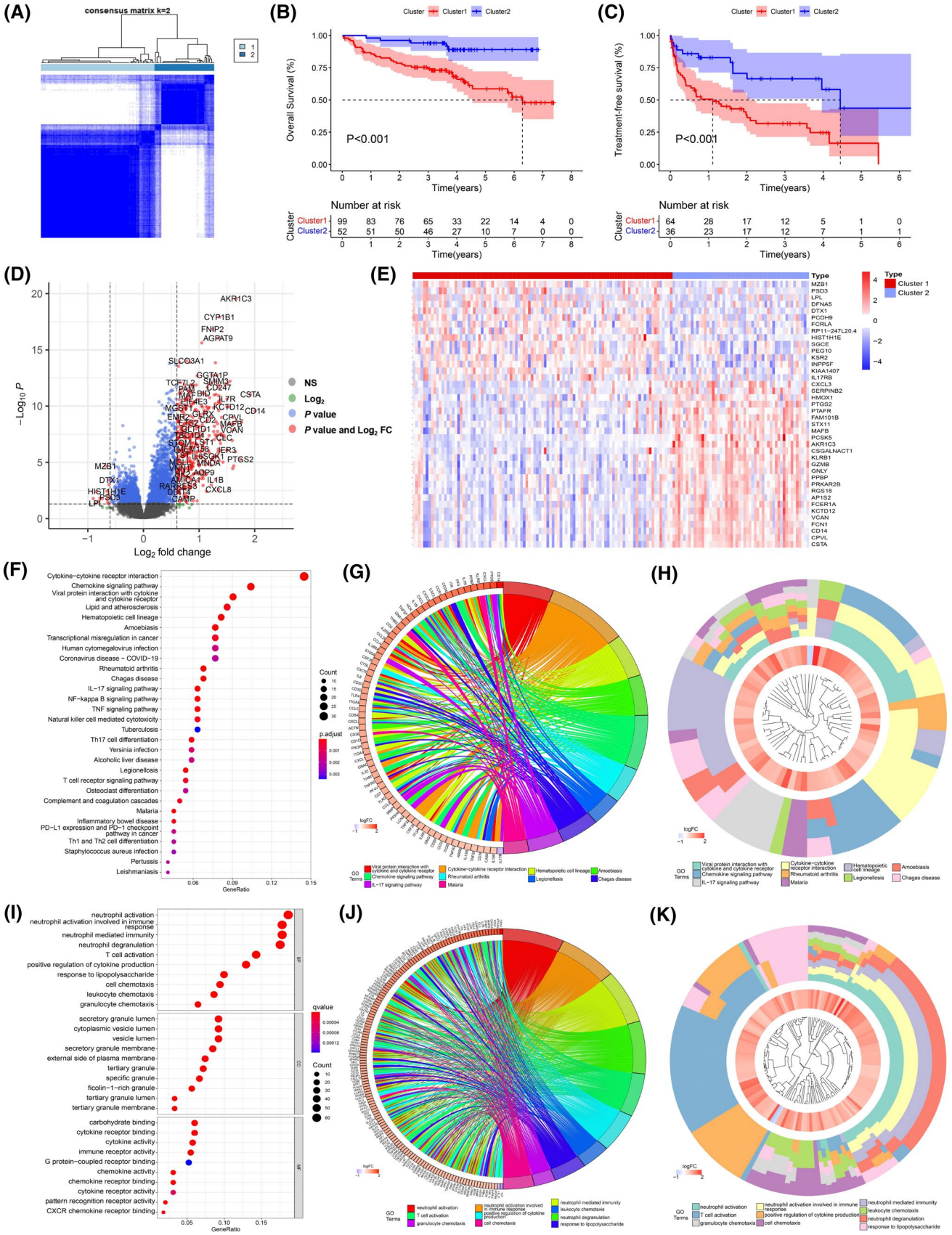
(A)
consensus matrix k=2
(B)
Cluster Cluster1 Cluster2
Overall Survival (%)
P<0.001
Time(years)
Number at risk
Cluster1 99 83 76 65 33 22 14 4 0
Cluster2 52 51 50 46 27 10 7 0 0
(C)
Cluster Cluster1 Cluster2
Treatment-free survival (%)
P<0.001
Time(years)
Number at risk
Cluster1 64 28 17 12 5 1 0
Cluster2 36 23 17 12 7 1 1
(D)
−Log10 P
Log2 fold change
NS
Log2
P value
P value and Log2 FC
AKR1C3
CYP1B1
FNIP2
AGPAT9
SLCO3A1
CSTA
CD14
MZB1
DTX1
HIST1H1E
PSD3
LPL
CXCL8
(E)
Type
Cluster 1
Cluster 2
MZB1
PSD3
LPL
DFNA5
DTX1
PCDH9
FCRLA
RP11−247L20.4
HIST1H1E
SGCE
PEG10
KSR2
INPP5F
KIAA1407
IL17RB
CXCL3
SERPINB2
HMOX1
PTGS2
PTAFR
FAM101B
STX11
MAFB
PCSK5
AKR1C3
CSGALNACT1
KLRB1
GZMB
GNLY
PPBP
PRKAR2B
RGS18
AP1S2
FCER1A
KCTD12
VCAN
FCN1
CD14
CPVL
CSTA
(F)
Cytokine−cytokine receptor interaction
Chemokine signaling pathway
Viral protein interaction with cytokine and cytokine receptor
Lipid and atherosclerosis
Hematopoietic cell lineage
Amoebiasis
Transcriptional misregulation in cancer
Human cytomegalovirus infection
Coronavirus disease − COVID−19
Rheumatoid arthritis
Chagas disease
IL−17 signaling pathway
NF−kappa B signaling pathway
TNF signaling pathway
Natural killer cell mediated cytotoxicity
Tuberculosis
Th17 cell differentiation
Yersinia infection
Alcoholic liver disease
Legionellosis
T cell receptor signaling pathway
Osteoclast differentiation
Complement and coagulation cascades
Malaria
Inflammatory bowel disease
PD−L1 expression and PD−1 checkpoint pathway in cancer
Th1 and Th2 cell differentiation
Staphylococcus aureus infection
Pertussis
Leishmaniasis
GeneRatio
Count
p.adjust
(G)
logFC
GO Terms
(H)
logFC
GO Terms
(I)
neutrophil activation
neutrophil activation involved in immune response
neutrophil mediated immunity
neutrophil degranulation
T cell activation
positive regulation of cytokine production
response to lipopolysaccharide
cell chemotaxis
leukocyte chemotaxis
granulocyte chemotaxis
secretory granule lumen
cytoplasmic vesicle lumen
vesicle lumen
secretory granule membrane
external side of plasma membrane
tertiary granule
specific granule
ficolin−1−rich granule
tertiary granule lumen
tertiary granule membrane
carbohydrate binding
cytokine receptor binding
cytokine activity
immune receptor activity
G protein−coupled receptor binding
chemokine activity
chemokine receptor binding
cytokine receptor activity
pattern recognition receptor activity
CXCR chemokine receptor binding
BP
CC
MF
GeneRatio
qvalue
Count
(J)
logFC
GO Terms
(K)
logFC
GO Terms

◂**Fig. 2** Two FA metabolism-related molecular phenotypes of CLL. **A** Unsupervised clustering analysis was used to divide patients into two different molecular clusters based on the expression of differentially expressed FA metabolism-related genes. **B**, **C**) Kaplan–Meier survival curves for OS and TFS of CLL patients into two molecular clusters. **D**, **E** Volcano and heatmap plots displayed the DEGs between different FA metabolism-related phenotypes. **F**–**H** KEGG functional enrichment analysis of the DEGs between two molecular clusters. **I**–**K** GO functional enrichment analysis of the DEGs between two molecular clusters

significantly worse OS ($P < 0.0001$) and TFS ($P < 0.0001$) (Fig. 5I, J). Moreover, the AUC values of the ROC curves for predicting the 1-, 3-, and 5-year OS were 0.786, 0.787, and 0.772, respectively, and 1-, 3-, and 5-year TFS were 0.760, 0.798, and 0.717 (Fig. 5K, L). In addition, Kaplan–Meier curves of the expression of 4 genes in FAPI are shown in Fig. S2, respectively.

Independence validation of the FAPI model

To further verify the FAPI model effectiveness, we applied the same formula mentioned above to calculate the FAPI score in 36 patients from our center as a validation cohort. The clinical characteristics are listed in Table S5. Kaplan–Meier curves of the expression level of AKR1C3, CYP1B1, GSTZ1, and HSD17B3 in the validation set are shown in Fig. S3, respectively. Survival status and risk score distribution of the validation cohort are shown in Fig. 6A, B, respectively. Like the GEO cohort, patients with higher FAPI levels were associated with poorer OS ($P < 0.0001$), PFS ($P = 0.0003$), and TFS ($P = 0.0071$, Fig. 6C–E). We performed AUCs of 1-, 3-, and 5-years OS, PFS, and TFS in Fig. 6F–H and indicated that the FAPI model has a satisfactory ability to assess the prognosis in CLL.

Meanwhile, the univariate analysis exhibited FAPI high risk ($P < 0.001$), Binet stage B or C ($P = 0.038$), B symptoms ($P = 0.045$), age > 65 years ($P = 0.047$), hemoglobin < 100 g/L ($P = 0.002$), β2-MG > 3.5 mg/L ($P = 0.011$), TP53 disruption ($P = 0.032$), IGHV unmutated ($P = 0.001$), and CLL International Prognosis Index (CLL-IPI) ($P < 0.001$) which were significantly correlated with inferior OS (Fig. 7A). Considering CLL-IPI included age, Binet stage, β2-MG, TP53 disruption, and unmutated IGHV, we only put FAPI, B symptoms, hemoglobin, and CLL-IPI in the multivariate analysis. The results demonstrated that FAPI ($P = 0.014$), hemoglobin < 100 g/L ($P = 0.012$), and CLL-IPI ($P = 0.034$) were independent prognostic indicators (Fig. 7B).

Construction nomogram models

Based on the result of multivariate analysis, a novel nomogram prognostic model was constructed by FAPI, hemoglobin, and CLL-IPI level, to predict 2-, 3-, and 5-year OS (Fig. 7C). The *C*-index of the nomogram model was 0.907. The nomogram calibration plots for 2-, 3-, and 5-year OS demonstrated an impressive relationship between the predicted and actual survival rates, suggesting that the nomogram model is a dependable tool for predicting the prognosis of patients with CLL (Fig. 7D–F).

Discussion

Currently, CLL-IPI prognostic model is mainly established based on the era of traditional immunochemotherapy [23]. In the era of new drugs, especially the era of chemo-free therapy, its guiding significance for clinicians to carry out personalized treatment is gradually being challenged. Metabolic reprogramming is a critical factor in the development of tumors. Tumor cells utilize environmental nutrients to sustain their survival and proliferation [24]. Accumulating evidence has delineated that dysregulated metabolism in cancer cells and tumor environment is of pivotal contribution to the cancer progression, treatment, recurrence, and metastasis, including FA metabolism. Therefore, targeting cancer metabolism has emerged as a promising approach in cancer research and therapy [25]. The endeavor to create prognostic signatures utilizing gene sets linked to distinct biological characteristics has been a pursuit within the field of cancer research. However, the specific involvement of FA metabolic reprogramming in CLL remains incompletely understood, and the essential molecular markers related to FA metabolism in CLL remain unclear [26].

This is the first study to investigate the relationship between genes involved in FA metabolism and CLL and has gained a more thorough comprehension of the function of these genes in CLL. Using univariate Cox regression analysis and LASSO Cox regression analysis, a prognostic risk score model of differentially expressed FA metabolism-related genes in CLL and normal samples was established in the GEO cohort. The prognostic risk score model was used to predict the outcome of CLL patients from the training set. There were survival disparities between CLL patients with low- and high-risk scores. The same outcome was reported in the validation set, indicating that the prognostic risk score model can identify patients with a poor prognosis for survival. In addition, the predictive power of this prognostic risk score model was enhanced by incorporating CLL-IPI into a risk assessment nomogram.

Two molecular clusters of CLL were identified based on the expression of 15 genes related to FA metabolism. Patients were accurately classified into these two clusters, with those in Cluster 1 having a significantly worse prognosis compared to those in Cluster 2. Analysis of intrinsic biological function was performed using differentially

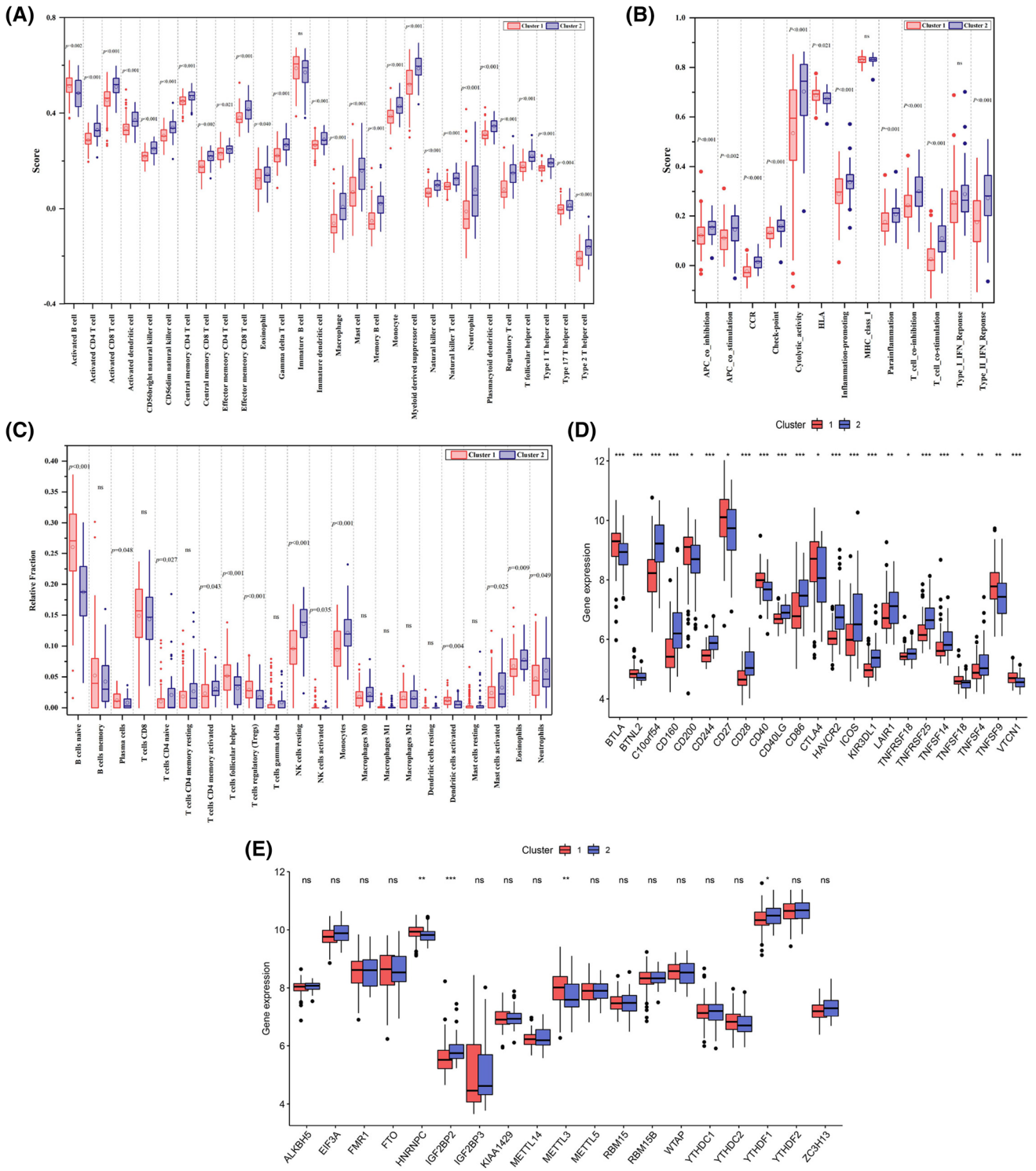

Fig. 3 Tumor immune microenvironment and m6A regulator analysis between different FA metabolism-related phenotypes. **A**, **B** The score of immune cell types and immune-related functions using ssGSEA analysis between two molecular clusters. **C** Boxplots of the relative fraction of 22 immune cell types between two groups. **D** The expression value of immune checkpoint genes between different FA metabolism-related phenotypes. **E** The expression value of m6A regulator genes between different FA metabolism-related phenotypes. (***$P < 0.001$; **$P < 0.01$; *$P < 0.05$; ns, no significance)

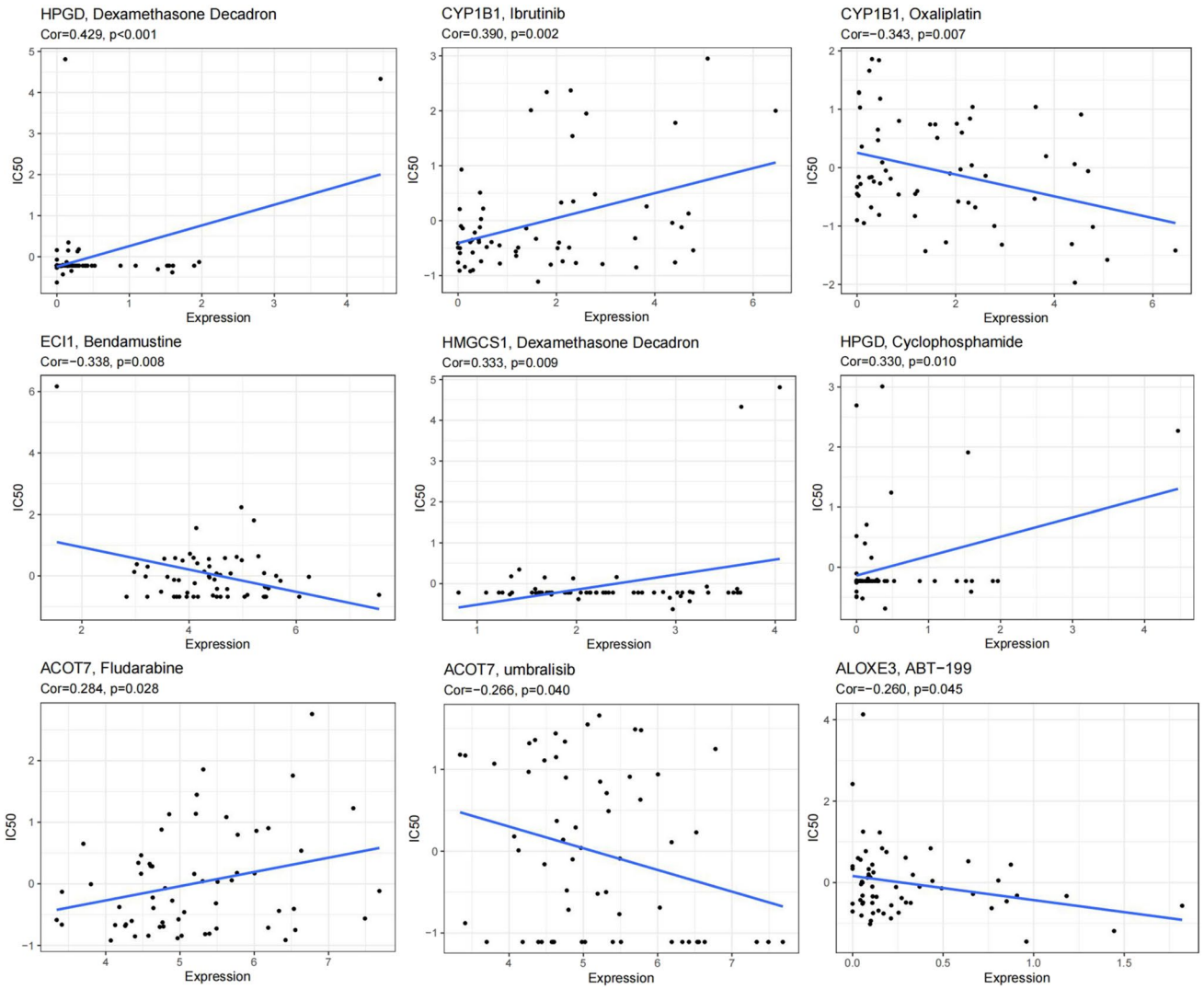

Fig. 4 The relationship between DEGs and common FDA-approved antineoplastic drug sensitivity by CellMiner database

expressed genes between two clusters, including the chemokine signaling pathway, IL-17 signaling pathway, NF-κB signaling pathway, PD-L1 expression and PD-1 checkpoint pathway in cancer, and T cell receptor signaling pathway. Chemokine signaling and FA metabolism are distinct biological processes that can exert mutual influence in various ways, frequently leading to significant implications for immunity and cancer. NF-κB pathway is constitutively activated in CLL and plays a major role in disease development and evolution [27]. It has been reported to play a key role in regulating the immune response to infection and inflammation [28]. Notably, it can interact with FA metabolism in several ways. For instance, it can induce the transcription of FA synthase (FASN) to catalyze the synthesis of long-chain saturated FA. Meanwhile, different types of FA can also modulate the NF-κB pathway. Studies have shown that saturated FA such as palmitate can activate the NF-κB pathway, leading to increased expression of inflammatory genes [29]. Our findings back up the involvement of the NF-κB signaling pathway in the metabolism of FAs in CLL.

FA metabolism influences the function of immune cells in TME, so it is worth exploring the differences in the degree of immune cell infiltration in our analysis of FA metabolism genes. As we expected, these data revealed a strong correlation between FA metabolism and immune-related pathways in CLL, which suggested that FA metabolism could be involved in TME remodeling. The immune function analysis demonstrated that Cluster 2 obtained higher scores both in immune inhibition and stimulation processes, checkpoint, cytolytic activity, and inflammation-promoting and IFN response. In addition, the prognostic risk was tightly related to immune cell infiltration. Our data also suggested that strong immunosuppressive TME was present in the FA metabolism high-risk group. The pivotal role of Tregs in the

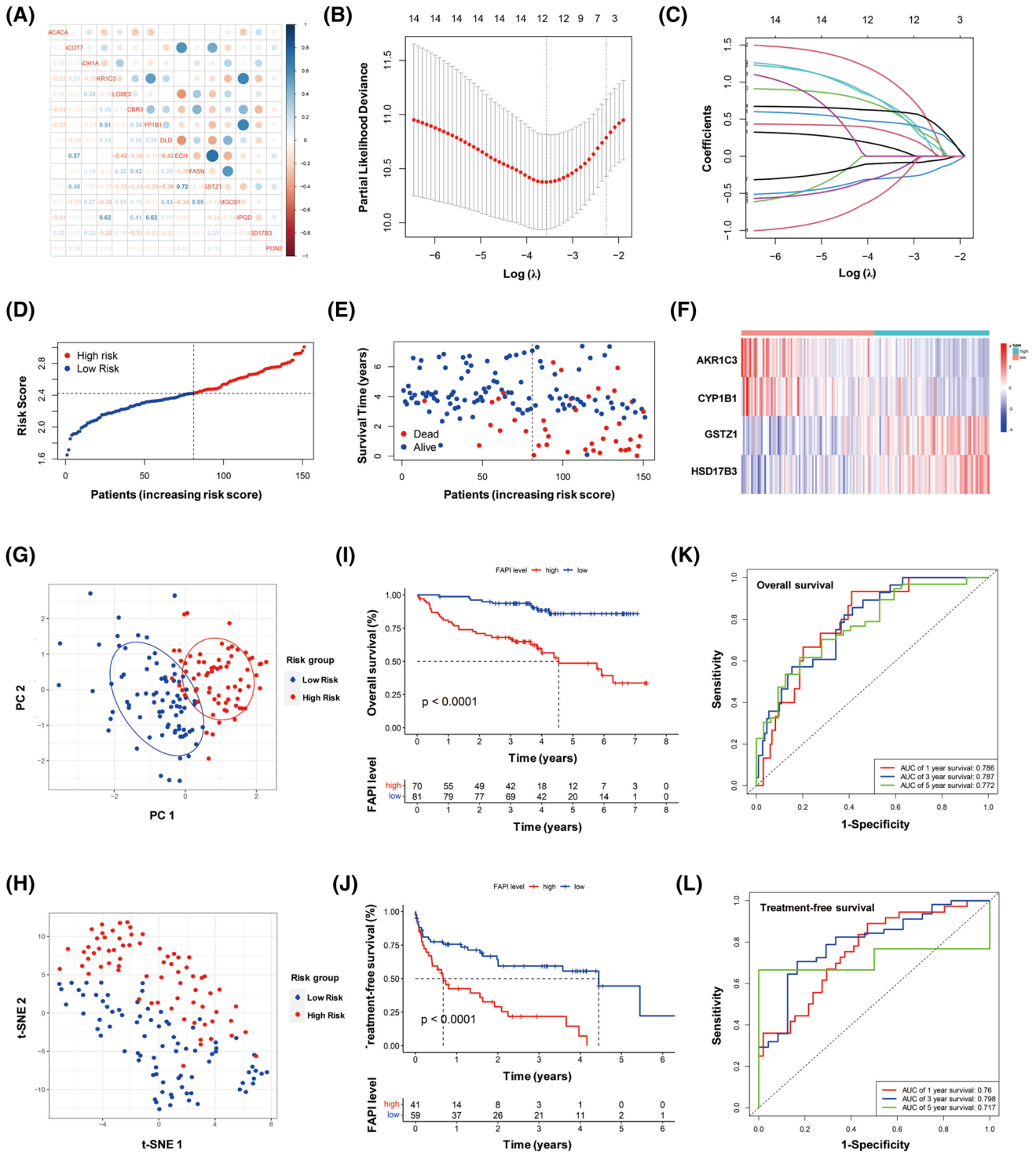

Fig. 5 Establishment and assessment of the novel prognostic model based on FA metabolism-related genes. **A** Correlation analysis of the 15 FA metabolism-related genes. **B** Four prognostic FA metabolism-related genes were identified by LASSO analysis based on optimal weight coefficients. **C** The LASSO coefficient profiles of the four genes signature. **D** The distribution and optimal cutoff value of risk scores in training cohort. **E** The distributions of OS status, OS, and risk score. **F** Heatmap of the expression of the four genes in prognostic model. **G**, **H** PCA and t-SNE analysis of the CLL visualizing the distribution of the low- and high-risk groups. **I**, **J** Kaplan–Meier survival curves for OS and TFS of FAPI model. **K**, **L** Time-dependent ROC curves of FAPI model for predicting the 1-, 3-, and 5-year OS and TFS

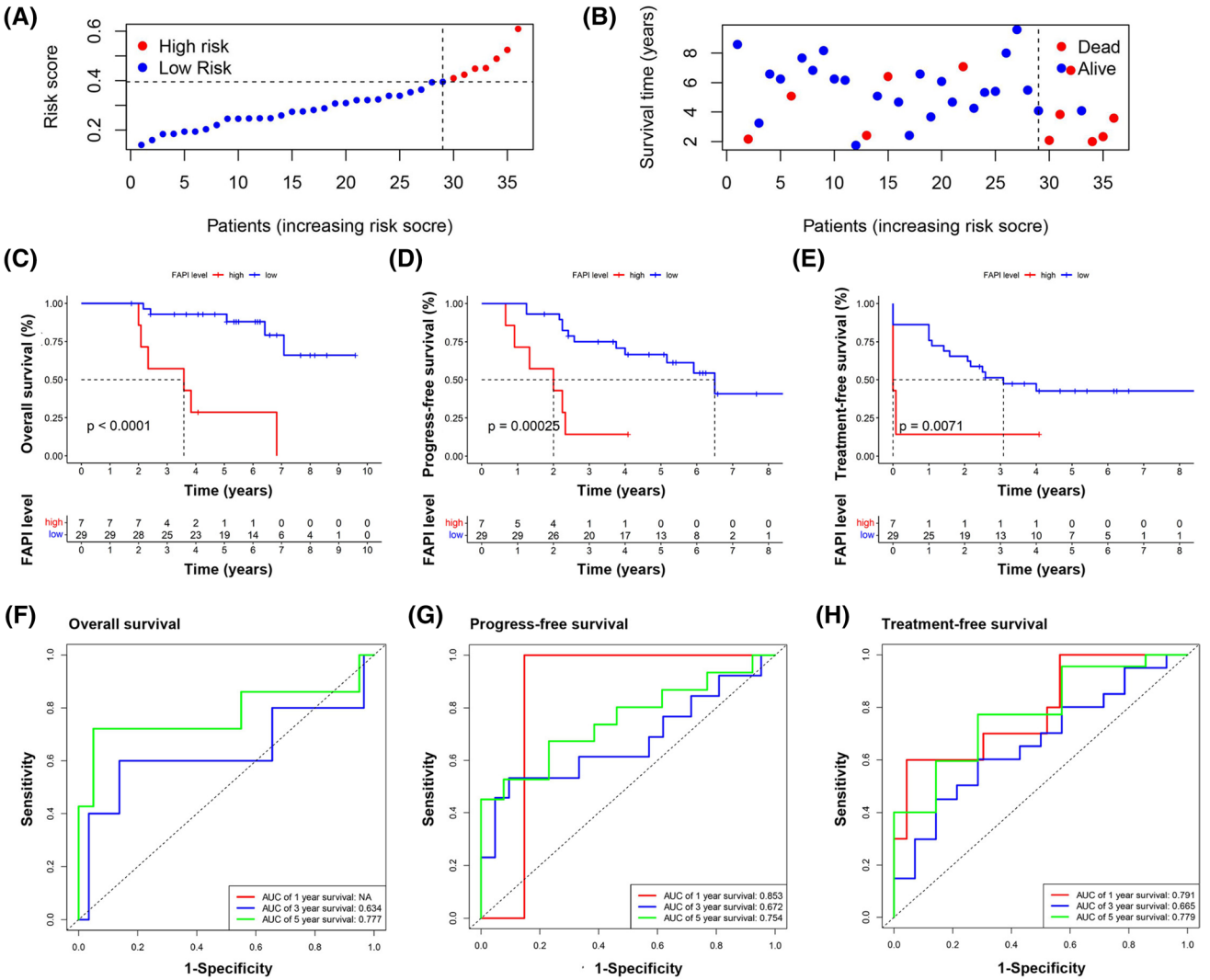

Fig. 6 Validation of the FAPI prognostic model. **A** The distribution and the value of risk scores in the validation cohort. **B** The distributions of OS status, OS, and risk score. **C–E** Kaplan–Meier survival curves for OS, PFS, and TFS of CLL patients stratified by FAPI risk score. **F–H** Time-dependent ROC curves of the risk model for predicting the 1-, 3-, and 5-year OS, PFS, and TFS

immunosuppressive TME with dysregulated FA metabolism is noteworthy, with significant differences in the enrichment of Tregs between the two clusters in CLL. Treg cells are more dependent on FA oxidation (FAO) under the metabolic stress of the TME [30]. Inhibition of FAO, attenuation of function, and reduction in the number of Tregs could be observed. As an important regulator of Treg development and function, FOXP3 can promote FA uptake and FAO and enhance Treg resistance to lipotoxic environments to allow for expansion [31]. Tregs may promote tumor survival and proliferation by suppressing anti-tumor immune responses. In 2011, Weiss et al. reported that high Treg levels are an indicator for predicting the time to initial treatment in patients with CLL in the low to intermediate stages [32]. Subsequent studies also have found that CLL is associated with profound defects in T cells and T cell functions, failing T cell antitumor activity [33]. Other reports also noted that the number and function of Tregs are often enhanced, which may help tumor cells evade attack by the immune system. Of note, in our study, although NK cell activation increased in the high-risk group, it did not necessarily predict a better anti-tumor effect. Previous studies indicated that increased lipid metabolism impairs NK cell function and mediates adaptation to the lymphoma environment [34]. This provided a plausible explanation for our results. We also observed neutrophil activation involved in immune response.

In recent years, immune checkpoint inhibitors (ICI), as an overall strategy of immunotherapy, have gradually become effective drugs for the treatment of tumors [35]. However, only a minority of patients benefit from ICIs targeting PD-1, PD-L1, or CTLA-4. We estimated the relationship between risk score and the immune checkpoints by comparing the

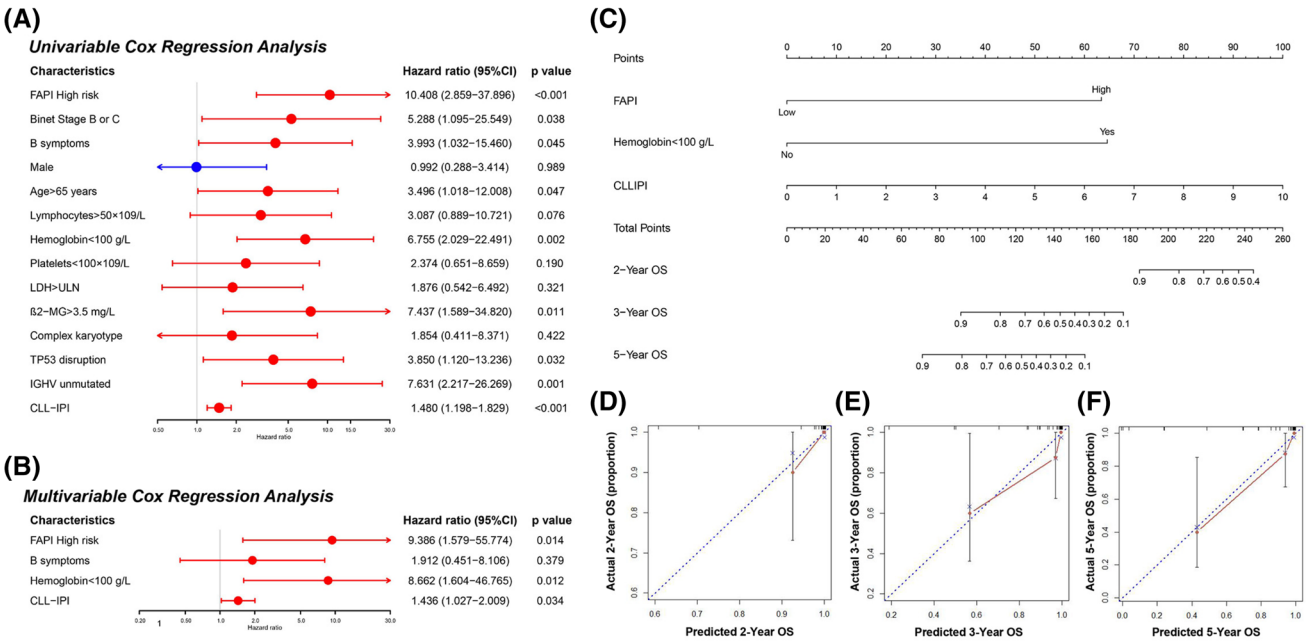

Fig. 7 Construction nomogram models. **A**, **B** The univariate and multivariate Cox regression model analyses of clinical characteristics and FAPI. **C** The nomogram model for predicting 2-, 3-, and 5-year OS rate of CLL patients. **D**–**F** The calibration plot analysis to assess the nomogram accuracy for OS prediction at 2-, 3-, and 5-year

expression levels of 47 selective immune checkpoints in CLL patients for potential implications for immunotherapy. These results showed that the expression levels of mostly targeted checkpoints were significantly amplified in Cluster 2, suggesting that a cluster of CLL patients may obtain stronger responses to treatments targeting these checkpoints. Among them, PD-1, PD-L1 and CTLA4 are hot star checkpoints as reported previously. We also observed some emerging immune checkpoints such as LAG3, ICOS, and TIGIT. These data are consistent with previously published articles showing that FA metabolism is important player in the immunosuppressive process of TME [34, 36]. These immune components of the TME plays different roles in various immune responses that promote or inhibit tumor survival. Different levels of immune cell infiltration and ICIs in the two subtypes may also cause patients to show different outcomes when receiving immunotherapy. Furthermore, tumor FA metabolism has been thought to be involved in resistance to chemotherapy, endocrine-targeted therapy, and radiotherapy. Cell membrane changes, energy changes, signal transmission, and anti-oxidation are all related to the response and resistance of tumor cells to chemotherapy drugs [37].

Notably, the FAPI model was established through LASSO Cox regression analysis. The reliability of the model can be partially confirmed by examining the roles of four metabolism-related genes in other diseases. AKR1C3 is a member of the aldo–keto reductase superfamily and is involved in the metabolism of steroid hormones and prostaglandins. It has been implicated in cancer progression and its mRNA expression was significantly higher in primary T-lineage ALL than B-lineage ALL. OBI-3424, an AKR1C3 inhibitor, can exert potent cytotoxicity against T-ALL cell lines and PDXs. It tends to be an inferior factor, which was consistent with our results [38]. CYP1B1 is primarily associated with the metabolism of estrogen and other endogenous compounds. It is expressed in several tissues, including the liver, adrenal glands, and various reproductive tissues. Moreover, GSTZ1 is responsible for the conversion of dichloroacetic acid to its inactive metabolite. It was significantly downregulated in sorafenib-resistant hepatoma cells and reduced the level of GSH, thereby inhibiting tumor progression via promoting sorafenib-induced ferroptosis in hepatocellular carcinoma tissues [39]. On the contrary, another study found that high expression of GSTZ1 was associated with poor prognosis in neuroblastoma, which may be due to the role of GSTZ1 in detoxification leading to resistance to chemotherapeutic drugs [40]. In CLL, our research shows the similar prognostic significance of GSTZ1 with glioblastoma and neuroblastoma other than breast cancer and hepatocellular carcinoma [39, 41]. Additionally, HSD17B3, primarily found in reproductive organs, is an enzyme that plays a key role in steroid biosynthesis, and its protein expression levels were significantly upregulated in primary and metastatic prostate cancer patients compared with non-tumor samples [42]. However, the biological role of HSD17B3 in hematological

malignancy remains poorly understood. In our study, elevated HSD17B3 was associated with inferior OS and PFS.

Overall, we performed a systematic analysis of FA metabolism in CLL and constructed a new nomogram prognostic model FAPI. Nevertheless, this study still contains some limitations. Due to the small number of samples in the external cohort and the internal validation cohort, this needs to be validated in more CLL patients. Additionally, we identified multiple FA metabolism-related molecules with prognostic significance, but lack of profound mechanism in CLL. The relationship between FA metabolism and immunosuppressive TME as well as drug resistance in CLL could be further explored. In conclusion, these findings can effectively guide clinical practice to achieve a more personalized clinical follow-up strategy, paving the way for the future development of personalized cancer chemotherapy and immunotherapy.

Supplementary Information The online version contains supplementary material available at https://doi.org/10.1007/s00277-023-05590-y.

Acknowledgements We would like to acknowledge the patients who volunteered to participate in this study and the Core Facility of the First Affiliated Hospital of Nanjing Medical University for their instructions.

Author contribution BP and ZX provided the study design. BP, ZX, and KD participated in writing the article and making figures and tables. JZ and RG were responsible for analyzing data and interpreting results. Sample collection and clinical data interpretation were completed by HS, JL, YL, LW, and JL. WX and JW provided instructions and revised the paper. Final approval of the manuscript was performed by all authors who contributed to the article.

Funding This research was funded by the National Natural Science Foundation of China (grant number 82200887), Jiangsu Science and Technology Department (grant number BK20220716), and China Postdoctoral Science Foundation (grant number 2022M711404).

Data availability The authors declare that all data and materials are available on request.

Declarations

Ethics approval and consent to participate The study was approved by the First Affiliated Hospital of Nanjing Medical University, Jiangsu Province Hospital. All procedures followed were in accordance with the ethical standards of the responsible committee on human experimentation (institutional and national) and with the Helsinki Declaration of 1975, as revised in 2008 (5). And written informed consent was obtained from all patients according to the Declaration of Helsinki.

Consent for publication Not applicable.

Competing interests The authors declare no competing interests.

References

1. Jemal A, Siegel R, Ward E, Murray T, Xu J, Thun MJ (2007) Cancer statistics, 2007. CA Cancer J Clin 57(1):43–66
2. Hallek M, Shanafelt TD, Eichhorst B (2018) Chronic lymphocytic leukaemia. Lancet 391(10129):1524–1537
3. Hallek M, Cheson BD, Catovsky D et al (2018) iwCLL guidelines for diagnosis, indications for treatment, response assessment, and supportive management of CLL. Blood 131(25):2745–2760
4. Sharma S, Rai KR (2019) Chronic lymphocytic leukemia (CLL) treatment: so many choices, such great options. Cancer 125(9):1432–1440
5. Moreno C, Mora A (2021) MRD in CLL: some answers, many questions. Blood 138(26):2746–2747
6. Hanahan D (2022) Hallmarks of cancer: new dimensions. Cancer Discov 12(1):31–46
7. Li Z, Zhang H (2016) Reprogramming of glucose, fatty acid and amino acid metabolism for cancer progression. Cell Mol Life Sci 73(2):377–392
8. Maher M, Diesch J, Casquero R, Buschbeck M (2018) Epigenetic-transcriptional regulation of fatty acid metabolism and its alterations in leukaemia. Front Genet 9:405
9. Bian X, Liu R, Meng Y, Xing D, Xu D, Lu Z (2021) Lipid metabolism and cancer. J Exp Med 218(1):e20201606
10. Jiang F, Luo F, Zeng N et al (2022) Characterization of fatty acid metabolism-related genes landscape for predicting prognosis and aiding immunotherapy in glioma patients. Front Immunol 13:902143
11. Pi M, Kuang H, Yue C et al (2022) Targeting metabolism to overcome cancer drug resistance: a promising therapeutic strategy for diffuse large B cell lymphoma. Drug Resist Updat 61:100822
12. Rozovski U, Hazan-Halevy I, Barzilai M, Keating MJ, Estrov Z (2016) Metabolism pathways in chronic lymphocytic leukemia. Leuk Lymphoma 57(4):758–765
13. Rozovski U, Grgurevic S, Bueso-Ramos C et al (2015) Aberrant LPL expression, driven by STAT3, mediates free fatty acid metabolism in CLL cells. Mol Cancer Res 13(5):944–953
14. Bertrand KA, Giovannucci E, Rosner BA, Zhang SM, Laden F, Birmann BM (2017) Dietary fat intake and risk of non-Hodgkin lymphoma in 2 large prospective cohorts. Am J Clin Nutr 106(2):650–656
15. Solans M, Castello A, Benavente Y et al (2018) Adherence to the Western, Prudent, and Mediterranean dietary patterns and chronic lymphocytic leukemia in the MCC-Spain study. Haematologica 103(11):1881–1888
16. Heintel D, Kienle D, Shehata M et al (2005) High expression of lipoprotein lipase in poor risk B-cell chronic lymphocytic leukemia. Leukemia 19(7):1216–1223
17. Van't Veer MB, Brooijmans AM, Langerak AW et al (2006) The predictive value of lipoprotein lipase for survival in chronic lymphocytic leukemia. Haematologica 91(1):56–63
18. Kaderi MA, Kanduri M, Buhl AM et al (2011) LPL is the strongest prognostic factor in a comparative analysis of RNA-based markers in early chronic lymphocytic leukemia. Haematologica 96(8):1153–1160
19. Prieto D, Oppezzo P. (2017) Lipoprotein lipase expression in chronic lymphocytic leukemia: new insights into leukemic progression. Molecules 22(12):2083
20. Xu W, Li JY, Shen QD, Wu YJ, Yu H, Fan L (2009) Expression level of lipoprotein lipase in Chinese patients with chronic lymphocytic leukemia and its correlation with other prognostic factors. Int J Lab Hematol 31(5):552–559
21. Gao R, Du K, Liang J, et al. (2023) Low serum cholesterol level is a significant prognostic factor that improves CLL-IPI in chronic lymphocytic leukaemia. Int J Mol Sci 24(8):7396
22. Gao R, Chen RZ, Xia Y et al (2018) Low T3 syndrome as a predictor of poor prognosis in chronic lymphocytic leukemia. Int J Cancer 143(3):466–477
23. International CLLIPIwg (2016) An international prognostic index for patients with chronic lymphocytic leukaemia

(CLL-IPI): a meta-analysis of individual patient data. Lancet Oncol. 17(6):779–790.
24. Yu Z, Zhou X, Wang X (2022) Metabolic reprogramming in hematologic malignancies: advances and clinical perspectives. Cancer Res 82(17):2955–2963
25. Martinez-Reyes I, Chandel NS (2021) Cancer metabolism: looking forward. Nat Rev Cancer 21(10):669–680
26. Nie Y, Yun X, Zhang Y, Wang X (2022) Targeting metabolic reprogramming in chronic lymphocytic leukemia. Exp Hematol Oncol 11(1):39
27. Mansouri L, Papakonstantinou N, Ntoufa S, Stamatopoulos K, Rosenquist R (2016) NF-kappaB activation in chronic lymphocytic leukemia: a point of convergence of external triggers and intrinsic lesions. Semin Cancer Biol 39:40–48
28. Taniguchi K, Karin M (2018) NF-kappaB, inflammation, immunity and cancer: coming of age. Nat Rev Immunol 18(5):309–324
29. Huang W, Man Y, Gao C et al (2020) Short-chain fatty acids ameliorate diabetic nephropathy via GPR43-mediated inhibition of oxidative stress and NF-kappaB signaling. Oxid Med Cell Longev 2020:4074832
30. Yang K, Wang X, Song C et al (2023) The role of lipid metabolic reprogramming in tumor microenvironment. Theranostics 13(6):1774–1808
31. Howie D, Cobbold SP, Adams E et al (2017) Foxp3 drives oxidative phosphorylation and protection from lipotoxicity. JCI Insight 2(3):e89160
32. Weiss L, Melchardt T, Egle A, Grabmer C, Greil R, Tinhofer I (2011) Regulatory T cells predict the time to initial treatment in early stage chronic lymphocytic leukemia. Cancer 117(10):2163–2169
33. Riches JC, Davies JK, McClanahan F et al (2013) T cells from CLL patients exhibit features of T-cell exhaustion but retain capacity for cytokine production. Blood 121(9):1612–1621
34. Kobayashi T, Lam PY, Jiang H et al (2020) Increased lipid metabolism impairs NK cell function and mediates adaptation to the lymphoma environment. Blood 136(26):3004–3017
35. Perez-Ruiz E, Melero I, Kopecka J, Sarmento-Ribeiro AB, Garcia-Aranda M, De Las RJ (2020) Cancer immunotherapy resistance based on immune checkpoints inhibitors: targets, biomarkers, and remedies. Drug Resist Updat 53:100718
36. Corn KC, Windham MA, Rafat M (2020) Lipids in the tumor microenvironment: from cancer progression to treatment. Prog Lipid Res 80:101055
37. Hoy AJ, Nagarajan SR, Butler LM (2021) Tumour fatty acid metabolism in the context of therapy resistance and obesity. Nat Rev Cancer 21(12):753–766
38. Evans K, Duan J, Pritchard T et al (2019) OBI-3424, a novel AKR1C3-activated prodrug, exhibits potent efficacy against preclinical models of T-ALL. Clin Cancer Res 25(14):4493–4503
39. Wang Q, Bin C, Xue Q et al (2021) GSTZ1 sensitizes hepatocellular carcinoma cells to sorafenib-induced ferroptosis via inhibition of NRF2/GPX4 axis. Cell Death Dis 12(5):426
40. Cheng B, Wang Y, Ayanlaja AA, et al (2022) Glutathione S-transferases S1, Z1 and A1 serve as prognostic factors in glioblastoma and promote drug resistance through antioxidant pathways. Cells 11(20):3232
41. Tang Y, Tian W, Xie J et al (2022) Prognosis and dissection of immunosuppressive microenvironment in breast cancer based on fatty acid metabolism-related signature. Front Immunol 13:843515
42. Bamodu OA, Tzou KY, Lin CD, et al (2021) Differential but concerted expression of HSD17B2, HSD17B3, SHBG and SRD5A1 testosterone tetrad modulate therapy response and susceptibility to disease relapse in patients with prostate cancer. Cancers (Basel) 13(14):3478